EPJ Web of Conferences **40**, 06003 (2013)
DOI: 10.1051/epjconf/20134006003

Structural and magnetic studies of the nanocrystalline Nd-Fe-B-Nb alloy ribbons

M. Szwaja[1], K. Pawlik[1], P. Pawlik[1], W. Kaszuwara[2], J. J. Wysłocki[1] and P. Gębara[1]

[1]Institute of Physics, Częstochowa University of Technology, Al. Armii Krajowej 19, 42-200 Częstochowa, Poland
[2]Department of Materials Engineering, Warsaw University of Technology, ul. Wołoska 141, 02-507 Warszawa, Poland

Abstract: A detailed studies of the phase constitution, microstructure and magnetic properties of the nanocrystalline $Nd_{9.2}Fe_{61.64}B_{21.16}Nb_8$ alloy ribbons, are reported. It was shown that the rapidly solidified ribbons have partially amorphous structure and soft magnetic properties in the as-cast state. The heat treatment at temperatures higher than 923 K led to the growth of the hard magnetic $Nd_2Fe_{14}B$ phase and the metastable $Nd_2Fe_{23}B_3$ phase. The Mössbauer confirmed that during annealing of the samples at temperature higher than 923 K the paramagnetic $Nd_{1+\varepsilon}Fe_4B_4$ phase was also formed. The microstructure consisting of mixture of constituent phases was observed with transmission electron microscopy (TEM). Furthermore, with increasing annealing temperature the decrease of the saturation polarization J_s was observed. The maximum values of coercivity ${}_JH_c$ = 1175 kA/m was obtained for a sample annealed at 1023K. However, annealing at 1003 K resulted in the improvement of remanence polarization J_r = 0.35 T and the maximum energy product $(BH)_{max}$ = 21 kJ/m^3.

1 Introduction

Permanent magnets are one of the key components of electromechanical, electronic and medical devices [1, 2]. Nanocrystalline RE-Fe-B-based magnets have attracted much attention since their discovery in 1984 [3, 4] and have been extensively studied until now. Much of the work carried out has been concentrated on Nd-Fe-B and Pr-Fe-B alloys [5-9], for their excellent magnetic properties. In recent years, most frequently used methods for production of magnets are rapid solidification techniques. In order to obtain optimal magnetic properties, appropriate chemical composition and suitable heat treatment, are crucial issues [5].

The effect of Nb admixture on microstructure and magnetic reversal process was studied in [6, 7] for sintered magnets. It was demonstrated in [7] that admixture of 1 at.% Nb to the $Nd_{4.5}Fe_{75.8}B_{18.5}Nb_1$ alloy resulted in refinement of the microstructure of nanocrystalline ribbons, thus leading to improvement of magnetic properties. Interesting properties were observed for Nd-Fe-B alloy doped with 4 at.% of Nb [8, 9], where processing of bulk nanocrystalline rods was possible by suitable annealing of amorphous precursors. Furthermore, it was shown in [10, 11] that large content of B influences the vitrification ability of alloys, while Nb addition has a significant impact not only on the glass forming abilities, but also on limiting the growth of nanocrystalline grains formed during annealing. The aim of present work was to determine the influence of the annealing conditions on the phase constitution, microstructure and magnetic properties of rapidly solidified ribbons of the $Nd_{9.2}Fe_{61.64}B_{21.16}Nb_8$ alloy.

2 Experimental

The ingot sample of nominal composition $Nd_{9.2}Fe_{61.64}B_{21.16}Nb_8$ was prepared from the high purity constituent elements with pre-alloyed Fe-B by arc-melting under an argon atmosphere. In order to get homogenous composition, the samples were remelted several times. Subsequently, ribbon samples were produced by melt-spinning technique under the Ar atmosphere. Here the linear speed of the copper roll surface of 35m/s was used. Subsequently the ribbon samples were sealed off in a quartz tube under low pressure of argon to maintain the purity of the atmosphere during heat treatment. In order to obtain a nanocrystalline microstructure, the samples were subjected to short time (5 min) annealing at temperatures ranging from 923K to 1063K.

The phase analysis was studied using X-ray diffractometry (XRD) with Cu Kα radiation. Hysteresis loops were measured by LakeShore 7307 vibrating sample magnetometer at external magnetic field up to 2T at room temperature. Transmission Mössbauer spectra were obtained on a constant acceleration spectrometer

which utilized a rhodium matrix Co^{57} surface and calibrated at room temperature with α-Fe foil. The Mőssbauer spectra analysis was carried out using the Normos software. The microstructure of the ribbons was revealed using transmission electron microscope (TEM).

3 Results and discussion

The diffraction patterns of as-cast and annealed $Nd_{9.2}Fe_{61.64}B_{21.16}Nb_8$ alloy ribbons, are shown in figure 1. One can see, that the as-cast ribbon has partially amorphous structure, as evidenced by a few peaks corresponding to crystalline phases. Too small intensity of these peaks comparing to the background does not allow clear identification of crystalline phases present in the samples. Short-time annealing of specimens (for 5 min) at 963K and higher temperatures resulted in significant changes of their crystalline structure. The volume fraction of amorphous phase decreases in expense of growing grains of crystalline phases.

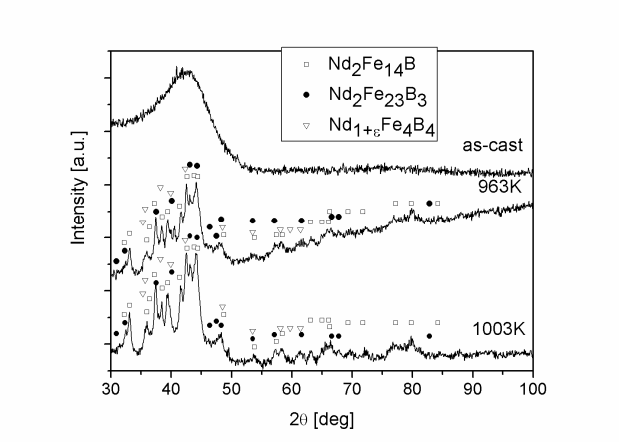

Fig. 1. X-ray diffraction patterns of $Nd_{9.2}Fe_{61.64}B_{21.16}Nb_8$ alloy ribbon sample in as-cast state and annealed at 963K and 1003K for 5 min.

The crystalline phases observed for the annealed ribbons were: the hard magnetic $Nd_2Fe_{14}B$, the paramagnetic $Nd_{1.1}Fe_4B_4$ and soft magnetic metastable $Nd_2Fe_{23}B_3$ phases [13]. Because of the overlapping of diffraction peaks corresponding to particular phases it was impossible to exactly identify them from the XRD scans. Therefore, for explicit phase analysis the Mőssbauer spectra were studied. The transmission Mőssbauer spectra of the $Nd_{9.2}Fe_{61.64}B_{21.16}Nb_8$ alloy ribbons in the as-cast state and annealed at 1003K for 5 min, are shown in figure 2.

The shape of the experimental data for the as-cast sample allowed to presume that it was mainly paramagnetic. Moreover, X-ray diffraction showed its amorphous structure with few not identified crystalline peaks. However, the shape of hysteresis loop measured for this specimen demonstrated its soft ferromagnetic behavior. Therefore, the best fitting of experimental data for as-cast sample was attained by taking into account two continuous components. The first one was a doublet, with quadrupole splitting distributions, corresponding to disordered paramagnetic phase. The next line was sextet, with hyperfine field distribution, related to ferromagnetic phase.

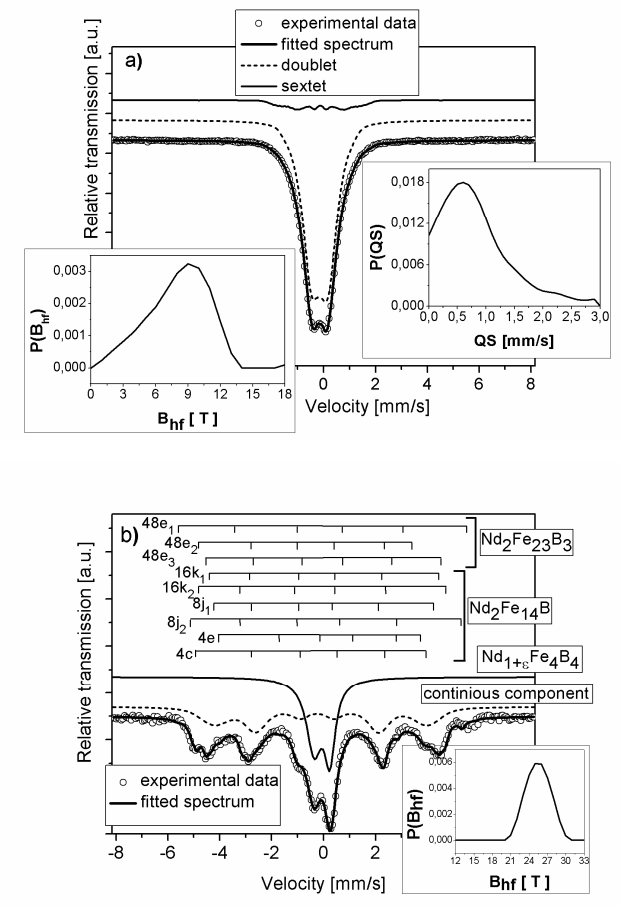

Fig. 2. Transmission Mőssbauer spectra of $Nd_{9.2}Fe_{61.64}B_{21.16}Nb_8$ alloy ribbon in as-cast state (a) and annealed at 1003K for 5 min (b) with hyperfine field and quadrupole splitting distributions

Annealing at 1003K for 5 min led to significant changes in shape of Mőssbauer spectra that suggest a presence a major fraction of crystalline phases. In fitting procedure of the experimental data, six Zeeman lines, corresponding to nonequivalent Fe atom positions ($16k_1$, $16k_2$, $8j_1$, $8j_2$, 4e, 4c) in the elementary cell of the $Nd_2Fe_{14}B$ hard magnetic phase [14, 15], were used. The soft magnetic $Nd_2Fe_{23}B_3$ phase [16, 17] was represented by three sextets with relative intensities ratio 1:1:1. Furthermore, a doublet was used to stand for paramagnetic $Nd_{1.1}Fe_4B_4$ phase [16, 17]. In the analysis of Mőssbauer spectra, a presence of amorphous or highly disordered phase in the phase constitution was represented by the continuous line. The quantitative analysis of this spectrum shown that ribbon annealed at 1003K for 5 min consists of 49 vol. % of the $Nd_{1.1}Fe_4B_4$ phase, 31 vol. % of the amorphous phase, 18 vol. % of the $Nd_2Fe_{14}B$ and 2 vol. % of the $Nd_2Fe_{23}B_3$ phases.

The microstructures of samples in as-cast state and subjected to annealing at 943K, 963K and 1003K were revealed by TEM.

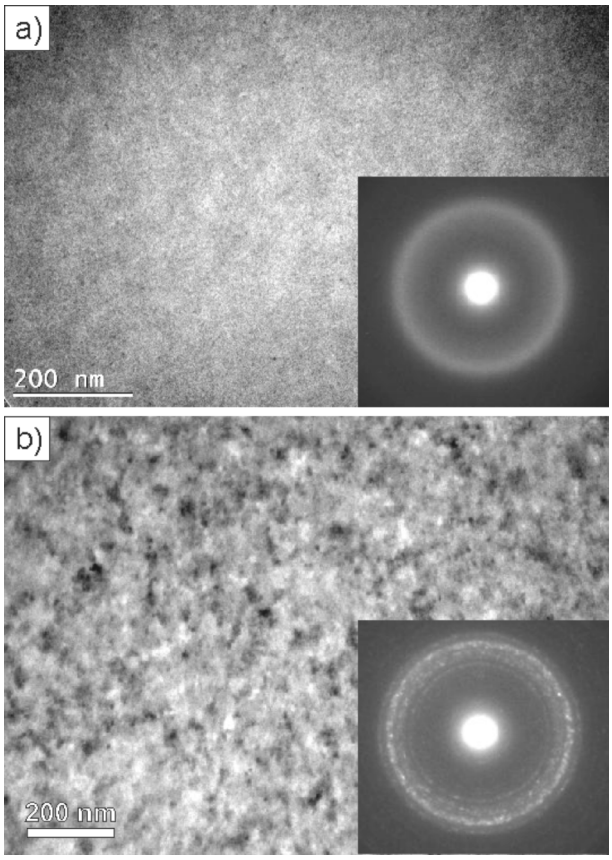

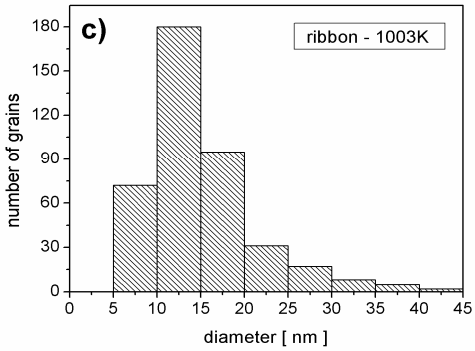

Fig. 3. Transmission electron micrographs of the $Nd_{9.2}Fe_{61.64}B_{21.16}Nb_8$ alloy ribbon sample in as-cast state (a) and annealed at 1003K (b) together with the electron diffraction pattern and the distribution of grains size measured for a series of images of the microstructure for ribbons annealed at 1003K (c)

The observed area of as-cast sample was fully amorphous. For the sample annealed at 943K the very fine grains of mean diameter ~ 10 nm were uniformly distributed within the amorphous matrix. Similar microstructure was observed for samples annealed at 963K and 1003K. The selected TEM image obtained for the ribbon annealed at 1003K accompanied by electron diffraction pattern are shown in figure 3b. The analysis of the electron diffractions for selected reflexes visible in the diffraction photograph for ribbon annealed at 1003K confirmed result obtained from XRD. Distribution of grain diameters for ribbon annealed at 1003K is shown in figure 3c. In both cases (ribbons annealed at 963K and 1003K) the average grain diameters were ~ 15 nm. However, the diffused ring visible on the electron diffraction pattern indicates presence of residual amorphous phase for these samples.

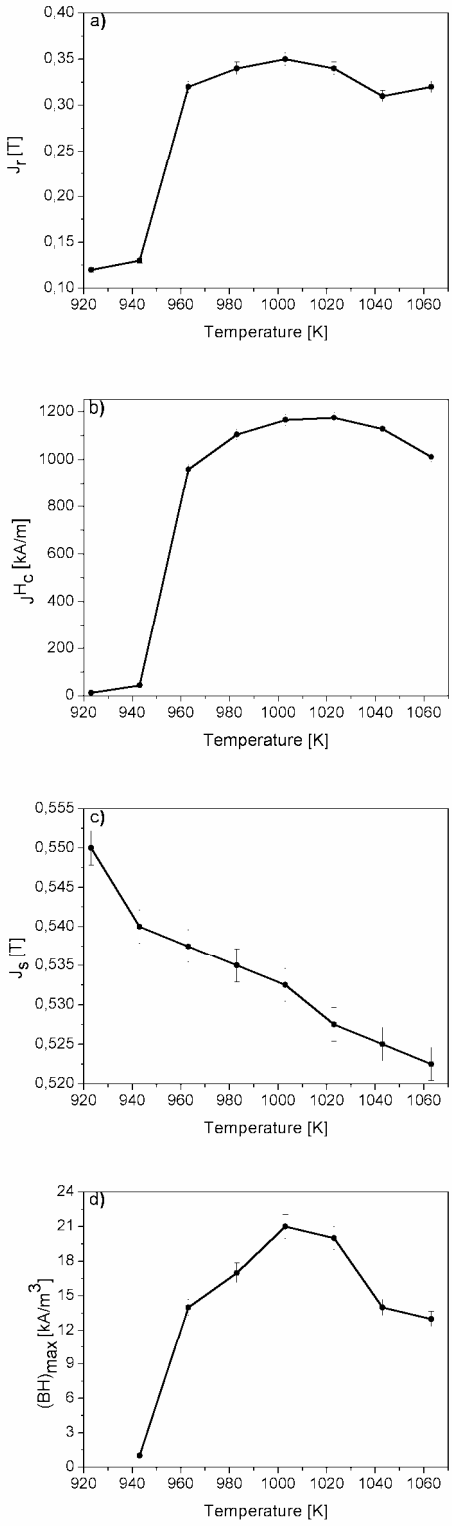

Fig. 4. The influence of annealing temperature on remanence polarization J_r (a), coercivity $_JH_c$ (b), saturation polarization J_s (c) and the maximum energy product $(BH)_{max}$ (d) of the $Nd_{9.2}Fe_{61.64}B_{21.16}Nb_8$ alloy ribbons annealed at the temperatures ranging from 923K to 1063K for 5 min.

For all the samples the magnetic properties were extracted from hysteresis loops measured at room temperature (figure 4 and 5).

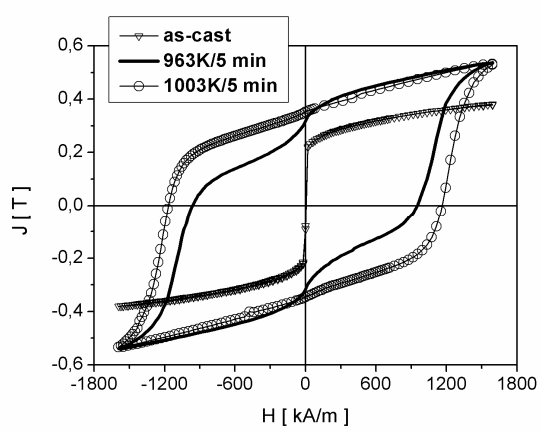

Fig. 5. The hysteresis loops measured for $Nd_{9.2}Fe_{61.64}B_{21.16}Nb_8$ alloy ribbon samples in the as-cast state and annealed at 963K and 1003K for 5 min.

With increasing annealing temperature the decrease of the saturation polarization J_s was observed. The reason of such decrease in J_s was coursed both by the low maximum field of measurements (up to 2T) and progressive increase in volume fraction of hard magnetic phase manifested by higher ${}_JH_c$. The maximum values of coercivity ${}_JH_c$ = 1175 kA/m was obtained for a sample annealed at 1023K. However, the heat treatment at 1003K exhibited the maximum values of remanence polarization J_r = 0.35 T and the maximum energy product $(BH)_{max}$ = 21 kJ/m^3.

4 Conclusions

In the present work, the structure and magnetic properties of the $Nd_{9.2}Fe_{61.64}B_{21.16}Nb_8$ alloy ribbons annealed at various temperatures from 923K to 1063K for 5 min, were investigated.

It was found that the as-cast $Nd_{9.2}Fe_{61.64}B_{21.16}Nb_8$ alloy ribbons, had partially amorphous structure and soft magnetic properties. Heat treatment of these ribbons led to growth of the hard magnetic $Nd_2Fe_{14}B$ phase, the paramagnetic $Nd_{1.1}Fe_4B_4$ and soft magnetic $Nd_2Fe_{23}B_3$ metastable phases. Short time annealing of the samples led to their very fine microstructure. The mean grain sizes ranging from 10 to 15 nm and do not change significantly with the annealing temperature. The rise of heat treatment temperature has an effect in the change of volume fractions of crystalline phases, which was reflected in the values of magnetic parameters. With increasing annealing temperature the decrease of the saturation polarization J_s was observed. The maximum values of coercivity ${}_JH_c$ = 1175 kA/m was obtained for a sample annealed at 1003K. However, annealing at 1023K resulted in the maximum value of remanence J_r = 0.35 T and $(BH)_{max}$ = 21 kJ/m^3. Furthermore, magnetic studies have shown that the heat treatment led to nanocrystalline structure of ribbons and good hard magnetic properties of the investigated materials.

Acknowledgements

Work supported by the research project N N507 240840 financed by Polish National Science Centre in years 2011-2014.

References

1. M. T. Thompson, *Practical Issues in the Use of NdFeB Permanent Magnets in Maglev, Motors, Bearings, and Eddy Current Brakes*, Procedings of the IEEE **97**, 1758 (2009)
2. J. I. Betancourt, Revista Maxicana De Fisica **48** (4), 283 (2002)
3. J. J. Croat, J. F. Herbst, R. W. Lee, F. E. Pinkerton, J. Appl. Phys. **55**, 2078 (1984)
4. M. Sagawa, S. Fujimura, N. Togawa, H. Yamamoto, J. Matsuura, J. Apel. Phys. **55**, 2083 (1984)
5. A. Manaf, R. A. Buckley, H. A. Davies, M. Leonowicz, J. Magn. Magn. Mat. **101**, 360 (1991)
6. D. Płusa, B. Wysłocki, J. Magn. Magn. Mater. **157**, 338 (1996)
7. D. H. Ping, K. Hono, H. Kanekiyo, S. Hirosawa, Acta Mater. **47**, 4641 (1999)
8. R. Tamura, S. Kobayashi, T. Fukuzaki, M. Isobe, Y. Ueda, J. Phys.: Conf. Ser. **144**, 012068 (2009)
9. M. Szwaja, P. Pawlik, J.J. Wysłocki, P. Gębara, Arch. Metall. Mater. **57**, 233 (2012)
10. J. Zhang, K. Y. Lim, Y. P. Feng, Y. Li, Scripta Materialia **56**, 943 (2007)
11. P. Pawlik, K. Pawlik, H.A. Davies, J.J. Wysłocki, W. Kaszuwara, J. Phys: Conf. Ser. **144**, 012060 (2009)
12. K. Pawlik, P. Pawlik, J.J. Wysłocki, Acta Phys. Pol A **118**, 900 (2010)
13. H. Mayot, O. Isnard, J.L. Soubezroux, J. Magn. Magn. Mater. **316**, e477 (2007)
14. F.E. Pinkerton, W.R. Dunham, Appl. Phys. Lett. **45** (11), 1248 (1984)
15. M. Yamasaki, M. Hamano, T. Kobayashi, Mater. Trans. **43**, 2885 (2002)
16. Z. Cheng, J. Shen, B. Zhang, M. Mao, J. Sun, Ch. Yang, F. Li, Y. Zhang, Chin. Phys. Lett. **14**, 387 (1997)
17. N. Tilijan, T. Zák, J. Stajić-Trošić, V. Menushenkov, Metalurgija- J.Metall. **8,** 201 (2002)